Quasi-particle self-consistent GW study of (Ga$_{1-x}$Al$_x$)$_2$O$_3$ alloys in the monoclinic and corundum structure

Amol Ratnaparkhe and Walter R. L. Lambrecht

Department of Physics, Case Western Reserve University, 10900 Euclid Avenue, Cleveland, OH 44106-7079, USA

The relative stability and energy of formation of the monoclinic and corundum structures which are respectively the lowest energy phases of Ga$_2$O$_3$ and Al$_2$O$_3$ are evaluated for mixed Ga-Al alloys. It is found that in the monoclinic structure, the Al has a strong preference for occupying the octahedral sites. The effects of alternate sites on the band structure and total energy are investigated. The band structures are calculated in the quasi-particle self-consistent GW approach.

1 Introduction β- Ga$_2$O$_3$ has drawn a lot of attention over the last few years as an emerging ultra-wide band gap semiconductor. It has a band gap of about 4.8 ± 0.1 eV but nevertheless is usually found to be n-type rather than insulating. This makes it attractive as a transparent conductive oxide (TCO) in photodiodes and photodetectors[1–3] in the UV region. Because a high band gap also leads to a high breakdown field, it has even more important potential applications in the area of high power electronics[4]. Many semiconductor devices require tailoring the band gap in a closely related material, to construct heterostructures. Thus it is of great interest to consider (Al$_x$Ga$_{1-x}$)$_2$O$_3$ alloys. Such alloys were already grown and incorporated in transistor devices,[5,6] and computationally studied.[7]

Both Ga$_2$O$_3$ and Al$_2$O$_3$ occur in different phases, among which the corundum structure or α-phase has the lowest energy for Al$_2$O$_3$ while the monoclinic β-phase has the lowest energy in Ga$_2$O$_3$. Thus the question naturally arises: what is the preferred structure in the alloy system as function of Al concentration? This question was already studied by Peelaers *et al.* [7] using hybrid functional [8,9] calculations. Here we re-investigate the question using the simpler generalized gradient approximation (GGA) functional in the Perdew-Burke-Ernzerhof (PBE) parametrization[10] to check to what extent their results are sensitive to the functional used. We find excellent agreement with their results.

Another important question for any alloys system is how to model the disordered arrangement of the two different cations on the cation sublattice. In the present case, it is important to note that in the corundum structure all cations are octahedrally coordinated, while the the monoclinic phase both octahedral and tetrahedrally coordinated sites occur. We will thus focus primarily on the occupation of these differently coordinated sites by Ga and Al atoms and their effects on the energy of formation and the band structure.

Finally, in order to obtain the most accurate band gaps, in a parameter free approach, we use here the quasiparticle self-consistent QSGW method.[11,12] Although the hybrid functional method also gives excellent band gaps they are to some extent adjusted to the experiment by choosing the fraction of exact exchange. In a previous study of β-Ga$_2$O$_3$[13] we found that the QSGW method significantly overestimates the gaps and required corrections for the missing electron-hole interactions in the calculation of the screened Coulomb interaction W as well as a lattice-polarization correction (LPC). Here we briefly revisit this question with better converged calculations in terms of **k**-point convergence and find the LPC effect is smaller than found in our previous work and essentially negligible.

2 Computational method The lattice constants and internal coordinates of the atoms in the cell were optimized within density functional theory (DFT) in PBE-GGA using the ABINIT plane wave pseudopotential approach. We used the Hartwigsen-Goedeker-Hutter (HGH)[14] pseudopo-

tentials from the ABINIT website and a plane wave cut-off of 50-70 Hartree and a $4 \times 4 \times 4$ mesh to sample the Brillouin zone.

Keeping the structures fixed, we then recalculated the total energies in the all-electron full-potential linearized muffin-tin orbital (FP-LMTO) method, [15, 16] which has the advantage to be free of pseudopotential choices. Further relaxation of the internal coordinates was found not to change the structure or total energy. A well converged double-κ smoothed Hankel function basis set was used with angular momentum cut-offs of $spdf\,spd$ and augmentation cut-off inside the sphere of $l_{max} = 4$. Ga-$3d$ semicore orbitals are included in the basis set as local orbitals (defined inside the muffin-tin sphere only). The Brillouin zone integrations of the total energy and self-consistency used a $6 \times 6 \times 6$ mesh. The band structures were calculated using the QSGW method[12] with most parameters chosen as in Ref. [13] except that we found it necessary to use a finer **k**-point mesh for the GW calculations in order to obtain well-converged self-energy corrections to the band gap. Specifically, we find that in order to have comparable convergence in the α and the β-structures, a mesh of $5 \times 5 \times 3$ is required for the latter and $4 \times 4 \times 4$ in the α structure. This gives the QSGW gaps converged to better than 0.1 eV.

All our reported gaps here include a fixed 0.8Σ correction. As discussed in detail in Bhandari *et al.* [17] and based on previous work, detailed in that paper, it is found that the QSGW method underestimates the macroscopic dielectric constants of semiconductors typically by 20 % and as a result overestimates the W and hence Σ self-energy or the gap correction between GW and LDA. Specifically, for a whole range of semiconductors, the experimental *vs.* calculated dielectric constants are linearly related but the slope is off by 20 % from exact agreement with each other. The origin of this underestimate of the screening has been clearly established to be the lack of electron-hole interaction diagrams in the calculation of the polarization propagator[18, 19] and can, among other, be corrected by including an exchange correlation kernel, schematically, $W = [1 - (v + f_{xc})P]^{-1}v$, or,[20, 21] more approximately by only including 80 % of the $\tilde{\Sigma} - v_{xc}^{LDA}$ in calculating the final band structures. Here $\tilde{\Sigma}_{ij} = \mathrm{Re}\{\Sigma_{ij}(\epsilon_i) + \Sigma_{ij}(\epsilon_j)\}/2$ is the energy independent and hermitian approximation to the $\Sigma(\omega)$ that is made self-consistent in QSGW. We note that this is quite different from the mixing of a fraction of exact exchange with LDA or GGA exchange used in hybrid functionals. The lattice polarization corrections are discussed in Sec. 4.1

3 Modeling of disorder Here we discuss the treatment of disorder. In principle, in an alloy one would need to consider an ensemble average over many different local configurations of the two different cations. One way to accomplish this is the special quasirandom structure (SQS) approach[22] in which one constructs the placement of the

different A and B atoms of a chosen size supercell such that various correlation parameters, such as different distance pair correlations and other local motifs all are as close as possible to the random ones. The idea is then that the energy of formation or other properties of interest can be expanded in a cluster expansion in terms of these correlations or local structural motifs and the random average is then well represented by this one carefully chosen structure. In metallic alloys, one typically needs to include various pair correlation functions in this treatment. However, in a semiconductor, one can argue that what matters most both for the total energy of bonding and for the band gap is the local coordination. For example, in a tetrahedrally coordinated semiconductor alloy with cation alloying, one could focus on the different tetrahedral environments of each anion, such as A_4, A_3B, A_2B_2, etc. Here we take this idea even one step further and assume that the properties will depend only on the relative occupation by the two atoms of the octahedral *vs.* tetrahedral sites. Within the 10 atom primitive cell of the β-structure, two cation sites are octahedral and two tetrahedral. Thus, we need to average in principle only over the probabilities that each site is occupied by Al or Ga. We hence calculate the total energies and band gaps for all possible occupations and then average them according to a Boltzman factor e^{-E/k_BT}. Now, if the energy differences between different sites are high compared even to the growth temperature, then it means the higher energy configurations will be strongly suppressed and we might as well assume only the lowest energy configuration occurs in the alloy. On the other hand, if the growth method is far from equilibrium, one could assume at the other extreme limit that the occupations are completely random. Specifically, for 25 % Al, the Al has then equal probability to be on a tetrahedral(t) or octahedral (o) site. Similar for 75 % the single Ga has equal probability to be on the tetrahedral or octahedral site. For 50 % there are 4 different configurations for the Al, tt, oo and two different to configurations. The two different to configurations differ depending on whether the two Al are next to each other or separated by a Ga in between. We thus need to check whether these have different energies (and gaps) or not. Assuming that they are close or that we neglect their difference than we would average the tt, to, oo configurations for the Al occupation with probabilities $1/4$, $1/2$, $1/4$ respectively. Our approach of considering all alloy configurations in a 10 atom cell is similar to Ref. [7] but somewhat more detailed analysis is provided here.

4 Results

4.1 Lattice polarization correction analysis Before addressing the alloys, we briefly review the accuracy of the QSGW method for the band gap of pure β-Ga$_2$O$_3$. Since our previous paper on β-Ga$_2$O$_3$, where we estimated the lattice polarization correction to the band gap to be as large as 0.5 eV, new insights were gained in Ref. [23]. Essentially the lattice polarization correction is now understood

as being a polaronic effect on the conduction band minimum (CBM) and valence band maximum (VBM) separately and depends on the effective masses of the latter, which sets the polaron length scale over which the effect is active, $a_P = \sqrt{\hbar/(2m_*\omega_L)}$, where ω_L is the longitudinal optical phonon. In a complete theory for multiple phonons, each phonon would come in with a contribution depending on the longitudinal projection of the corresponding eigenvector. Here we only wish to make an estimate of the upper limit of this effect. Assuming only the highest optical phonons matter (because they have the shortest a_P), these are of order 760 cm^{-1} in Ga$_2$O$_3$ [24] and using a hole effective mass of $2m_e$, the polaron length scale for holes is about 8.5 a_0. The estimated effect on the VBM shift is then $(e^2/4a_P)(\epsilon_\infty^{-1} - \epsilon_0^{-1})$ which amounts to about 0.07 eV with the factor $(\epsilon_\infty^{-1} - \epsilon_0^{-1})$ being about 0.17. The corresponding shifts of the CBM is smaller because the mass is much smaller ($\sim$0.2-0.3) and the polaron length is about 22 a_0. Thus we estimate the total effect must be smaller than 0.1 eV because this assumed the highest phonon fully contributed the maximal effect. Alternatively we can calculate the effect explicitly by adding a Lyddane-Sachs-Teller correction factor $\epsilon_0/\epsilon_\infty$ to the macroscopic dielectric constant at the $q = 0$ point singularity of the screened Coulomb interaction. However, because we apply this correction only at $q = 0$, that point must represent a region of q-space of size $1/a_P$. In fact, $1/a_P$ (averaged over electrons and holes) gives a **q**-point spacing of about 0.04 a_0^{-1} and this amounts to about 1/10 -th of the Brillouin zone in the ab plane. We find that with a $5\times5\times3$ mesh, adding this correction factor to the W at $q = 0$ reduced the gap by 0.1 eV. But clearly this must still be an overestimate because an even finer mesh is required to make $\Delta q \approx 1/a_P$. Hence, both estimates show clearly that the Fröhlich electron-phonon coupling effect on the gap must be less than 0.1 eV. It shows that in our previous work[13] where an insufficient **k**-point sampling $(4 \times 4 \times 2)$ was used, the effect was overestimated. Thus we conclude that we can safely neglect the electron-phonon effects on the gap but need a sufficiently fine GW **k**-point mesh. This then indeed gives a gap of 4.9 eV, for pure β-Ga$_2$O$_3$ in good agreement with experiment and no further corrections are needed for the alloys from this effect.

4.2 Lattice constants We first show the calculated pseudocubic lattice constants $V^{1/3}$ where V is the volume per formula unit of the alloys as function of Al concentration x in Fig. 1 for both structures. Here we used the structure with lowest energy in terms of the different Al occupations. We can clearly see that the lattice constants vary linearly with composition, in other words, they obey Vegard's law. Secondly, we see that the lattice constant is systematically smaller for the corundum than for the monoclinic phase. This is related to the octahedral only and mixed octahedral/tetrahedral coordination in corundum/monoclinic structures respectively.
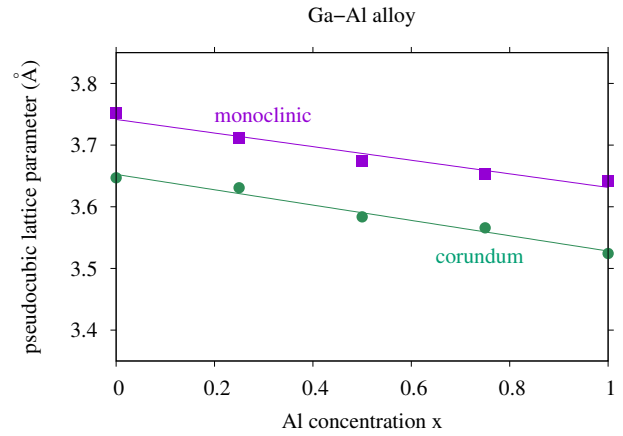

Figure 1 Pseudocubic lattice parameter of $(Al_xGa_{1-x})_2O_3$ as function of x for both crystal structures.
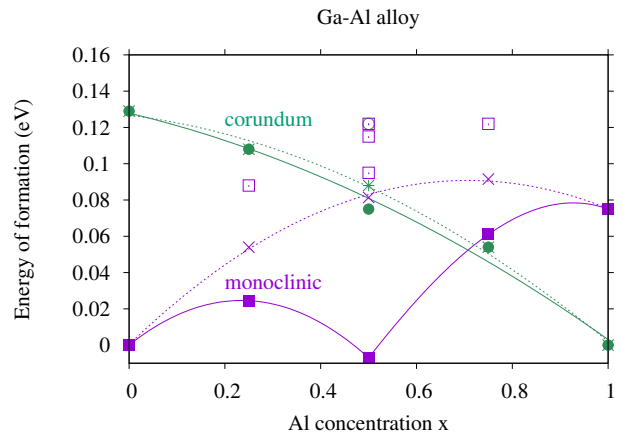

Figure 2 Energy of formation per formula unit for the alloys in the two structures across compositions. Solid data points show Al atoms occupying the octahedral positions while the higher energy hollow data points show the energies for configurations with increasing number of Al occupying tetrahedral sites. The $\times$ and $*$ show the average formation energies assuming random probability of the different configurations. The dotted lines show the corresponding interpolation while the solid lines assume the minimum energy configuration at each composition.

4.3 Energy of formation Next, we present the energies of formation, which are defined by

$$E_f[(Al_xGa_{(1-x)})_2O_3] = E[(Al_xGa_{(1-x)})_2O_3] \\ - xE[\alpha Al_2O_3] \quad (1) \\ - (1-x)E[\beta Ga_2O_3]$$

in Fig. 2. Please note that the reference energies of pure Ga$_2$O$_3$ and pure Al$_2$O$_3$ here are each calculated in their own lowest energy phase, whereas the alloy either can be in the α- or β-phase. This ensures that at the end points

Table 1 Energy of formation per formula unit and band gaps in different configurations as function of concentration in $(Al_xGa_{1-x})_2O_3$ alloys. In the monoclinic structure the configuration is specified by which atoms go in the octahedral (o) and tetrahedral (t) sites In the corundum structure, the sites are all octahedral but we can still distinguish the corner (c) and middle (m) sites in the structure.

x	Config.	ΔE_f (meV)	E_g (eV)
	monoclinic structure		
	t-o-o-t		
0.00	Ga-Ga-Ga-Ga	0	4.91
0.25	Ga-Ga-Al-Ga	20	5.48
0.25	Al-Ga-Ga-Ga	88	5.64
0.50	Ga-Al-Al-Ga	−7	6.16
0.50	Al-Ga-Ga-Al	122	6.30
0.50	Al-Al-Ga-Ga	95	6.20
0.50	Ga-Al-Ga-Al	116	6.25
0.75	Al-Ga-Al-Al	122	6.82
0.75	Al-Al-Al-Ga	61	6.87
1.00	Al-Al-Al-Al	75	7.74
	corundum structure		
	c-m-m-c		
0.00	Ga-Ga-Ga-Ga	129	5.28
0.25	Al-Ga-Ga-Ga	108	5.74
0.25	Ga-Ga-Al-Ga	108	5.74
0.50	Al-Ga-Ga-Al	79	6.72
0.50	Ga-Al-Al-Ga	79	6.72
0.50	Al-Ga-Al-Ga	75	6.41
0.50	Al-Al-Ga-Ga	122	6.79
0.75	Al-Al-Ga-Al	54	7.40
0.75	Al-Al-Al-Ga	54	7.40
1.00	Al-Al-Al-Al	0	8.88

$x = 0$ the monoclinic energy of formation is zero while at $x = 1$ the corundum one is equal to zero. All of the total energies are per formula unit. We first consider only the lowest energy configuration at each composition, which for the β structure amounts to placing Al preferentially on octahedral sites. The results are in excellent agreement with those of Peelaers *et al.* [7] if we assume that the latter contains a typo in that the energies of formation here are per formula unit and not per cation. It is clear from the results that the Al strongly prefers to occupy the octahedral site. The energy difference per Al_t going on a tetrahedral site however is not constant. The energy difference at the 50 % concentration $\Delta E_{to} = E_{to} - E_{oo}$ is not equal to that of $E_t - E_o$ at 25 %, where only one Al needs to choose between a tetrahedral and octahedral site and the energy difference $E_{tt} - E_{to} \neq E_{to} - E_{oo}$. This indicates that other aspects of the local configuration do play a role besides the nearest neighbor coordination.

The fact that the energy of formation in the monoclinic structure has a non-monotonic, bimodal distribution is interesting, in particular that the energy of formation even has a slightly negative value at 50 % is remarkable. The lower energy for adding two Al instead of one may in part be because this is a more symmetricstructure. The two Al

both on octahedral sites are related by the mirror plane symmetry perpendicular to the **b**-axis. The low energy of formation is clearly related to the optimum octahedral surrounding of Al combined with tetrahedral surrounding for Ga. Strictly speaking, the negative value of the energy of formation for this configuration indicates that the 50 % compound with all Al occupying octahedral sites is a separate crystalline phase distinct from a disordered alloy and would constitute a new compound on the convex hull in the ternary phase diagram.

To further study the effects of the Al distribution, we calculated the energy of formation and the band gaps for different configurations as shown in Table 1. These results are also shown as open symbols in Fig.2. We can see here that for the 50 % composition, four different Al distributions can be considered in the unit cell. Both Al on octahedral site, both on tetrahedral site and two different ways of one Al octahedral and one tetrahedral. The latter two differ in that in one case, the octahedral and tetrahedral are next to each other along the **b**-direction, while in the other case, there is Ga in between them. We can see that both of these have an energy of formation in between the fully tetrahedral or fully octahedral one but are still slightly different. Also, the energy cost of moving one Al from an octahedral to a tetrahedral site is not equal to half the energy for moving two of them. This again indicates that other aspects in the Al distribution play a role in the energetics, such as how close the Al containing octahedra or tetrahedra are to each other.

In the corundum structure, we have only octahedral sites but nonetheless we can define different sites in the unit cell and consider the effects of which ones are occupied by Al or Ga. The differences in energy of formation as well as band gap between the different configurations are much smaller in this case. The only exception is the case of two Ga atoms next to each other in the 50 % case, which has a 43 meV/formula unit higher energy. This may be because the two larger atoms are next to each other causes more distortion in the structure.

From Fig. 2, we can see that the $(Al_x\text{-}Ga_{(1-x)})_2O_3$ prefers to be in the monoclinic phase up to 70% Al concentration and the corundum phase thereafter. This however corresponds to the assumption that at each alloy composition the Al distribution is relaxed so the Al find their lowest energy configuration. If a random occupation would occur, modeled by the average energies of each possible configuration in the 10 atom cell the dotted lines are obtained in Fig. 2. Under that assumption the crossing to corundum phase would occur at lower concentration of Al. Nonetheless, from a thermodynamic point of view when comparing the relative stability of the two structures on the basis of energy, the assumption of minimizing the energy among different configurations is the more natural assumption. Since the total energy differences between the different configurations in Fig. 2 is of order 0.1 eV/formula unit, the Boltzmann factors for the higher energy configurations
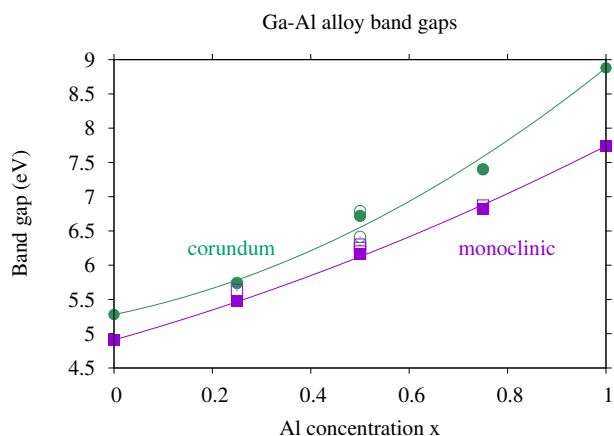
Ga-Al alloy band gaps

Figure 3 Direct band gap for the alloys as function of composition for each of the crystal structures. The solid symbols correspond to the lowest energy structure. The lines are a fit to these points with the parabolic equation definint the bowing coefficient. The open symbols to different configurations as detailed in Table 1.

with tetrahedral Al occupations would be about $e^{-1} = 0.37$ for a growth temperature of 1200K. This means the higher energy configurations are not expected to make a sizable contribution to the energy of formation.

4.4 Band gaps Next, we consider the band gaps as function of concentration in each phase in Fig. 3. In this plot we show the band gap in the alloy configuration with the lowest energy of formation as solid symbols and the line is interpolated through them. We can see that the gaps are systematically higher in the α than in the β structure but the difference increase with Al-concentration x. The band gaps do not vary linearly but the amount of band gap bowing is moderately small. Using the usual bowing equation $E_g(x) = xE_g^{Al} + (1-x)E_g^{Ga} - bx(1-x)$, the bowing coefficient b is 0.8 ± 0.1 eV for the β-phase, and 2.1 ± 0.3 eV for the α-phase by fitting this equation to the data points for the lowest total energy configuration.

Next we consider the band gap differences for different Al sites reported in Table 1. These are indicated as open symbols in Fig. 3 and show the slight variation of the gaps due to fluctuations in the local configuration. For the β phase, we can see that the gap is the smallest in the lowest energy structure of fully octahedrally coordinated Al but differs only by 0.14 eV from the highest energy configuration of both tetrahedral Al. The same is true for the 25 % Al case. In the 75 % case, the gaps are within 0.05 eV for both configurations. At 50 % we can see that when the two Al are adjacent to each other the gaps are slightly lower than when they are separated by a Ga. This is true both when the two Al are on adjacent tetrahedral sites and when they are on adjacent tetrahedral-octahedral sites.

Thus the band gaps differ only very slightly depending on the precise configuration. This is even more so for the

corundum structure. Hence the band gap bowings in Fig.3 obtained from the minimum energy configuration are adequate and a more random distribution will not lead to significantly larger or smaller bowing. Even when assuming completely random, non-equilibrium distribution of the Al, the band gaps will at most differ by 0.1 eV.

Overall, our band gaps are in good agreement with those of Ref. [7] obtained using a hybrid funtional with adjusted exact exchange fraction for the two end compounds. They are thus also in good agreement with the available experimental data.[7]

5 Conclusions In this paper we have studied the energy of formation and structural preference of $(Al_xGa_{1-x})_2O_3$ alloys in both corundum and monoclinic structures. In agreement with previous work based on hybrid functionals, we find that also with GGA the monoclinic structure is preferred up to about 70 % when the Al is allowed to find its lowest energy configuration. The energy of formation referred to the two end compounds each taken in their own lowest energy phase is bimodal in the monoclinic structure when assuming that the Al preferentially occupy the lowest energy octahedral sites when substituting for Ga. At 50 % it leads even to a slightly negative energy of formation indicating a new stable compound at 50 %. Other coordinations of Al have significantly higher energy in the β structure, in fact higher than in the corundum structure. Such configurations might nonetheless occur in case of non-equilibrium growth. Further study of the different configurations of how the Al are distributed in the primitive cell of the β or corundum structure, show that other factors may play a role in the energetics than simply octahedral *vs.* tetrahedral coordination. Depending on whether the growth the alloy is equilibrated or random, the concentration at which corundum becomes the preferred structure could vary from about 70 % to 50 %. Nonetheless, the band gaps here calculated at the QSGW level vary only within about 0.1 eV due to these different configurations. The band gaps show moderate bowing in both structures and are systematically higher and have a stronger bowing in the corundum structure. The QSGW method is here shown to give accurate band gaps without adjustable parameters for both end compounds and does not require a significant electron-phonon correction due to lattice polarization. This conclusion results from a re-evaluation of this effect and using a better converged **k**-point mesh in calculating the GW self energy compared with our previous work on β-Ga$_2$O$_2$.[13]

References

[1] Y. Kokubun, K. Miura, F. Endo, and S. Nakagomi, Applied Physics Letters **90**(3), 031912 (2007).

[2] R. Suzuki, S. Nakagomi, and Y. Kokubun, Applied Physics Letters **98**(13), 131114 (2011).

[3] S. Nakagomi, T. Momo, S. Takahashi, and Y. Kokubun, Applied Physics Letters **103**(7), 072105 (2013).

[4] K. Sasaki, M. Higashiwaki, A. Kuramata, T. Masui, and S. Yamakoshi, J. Cryst. Growth **378**, 591 – 595 (2013), The 17th International Conference on Molecular Beam Epitaxy.

[5] E. Ahmadi, O. S. Koksaldi, X. Zheng, T. Mates, Y. Oshima, U. K. Mishra, and J. S. Speck, Applied Physics Express **10**(7), 071101 (2017).

[6] P. Vogt, A. Mauze, F. Wu, B. Bonef, and J. S. Speck, Applied Physics Express **11**(11), 115503 (2018).

[7] H. Peelaers, J. B. Varley, J. S. Speck, and C. G. Van de Walle, Applied Physics Letters **112**(24), 242101 (2018).

[8] J. Heyd, G. E. Scuseria, and M. Ernzerhof, J. Chem. Phys. **118**(18), 8207–8215 (2003).

[9] J. Heyd, G. E. Scuseria, and M. Ernzerhof, J. Chem. Phys. **124**(21), 219906 (2006).

[10] J. P. Perdew, K. Burke, and M. Ernzerhof, Phys. Rev. Lett. **77**(18), 3865–3868 (1996).

[11] M. van Schilfgaarde, T. Kotani, and S. Faleev, Phys. Rev. Lett. **96**(22), 226402 (2006).

[12] T. Kotani, M. van Schilfgaarde, and S. V. Faleev, Phys.Rev. B **76**(16), 165106 (2007).

[13] A. Ratnaparkhe and W. R. L. Lambrecht, Applied Physics Letters **110**(13), 132103 (2017).

[14] C. Hartwigsen, S. Goedecker, and J. Hutter, Phys. Rev. B **58**(Aug), 3641–3662 (1998).

[15] M. Methfessel, M. van Schilfgaarde, and R. A. Casali, A Full-Potential LMTO Method Based on Smooth Hankel Functions, in: Electronic Structure and Physical Properties of Solids. The Use of the LMTO Method, edited by H. Dreyssé, , Lecture Notes in Physics Vol. 535 (Berlin Springer Verlag, 2000), , 114.

[16] T. Kotani and M. van Schilfgaarde, Phys. Rev. B **81**(12), 125117 (2010).

[17] C. Bhandari, M. van Schilgaarde, T. Kotani, and W. R. L. Lambrecht, Phys. Rev. Materials **2**(Jan), 013807 (2018).

[18] B. Cunningham, M. Grüning, P. Azarhoosh, D. Pashov, and M. van Schilfgaarde, Phys. Rev. Materials **2**(Mar), 034603 (2018).

[19] A. L. Kutepov, Phys. Rev. B **95**(May), 195120 (2017).

[20] W. Chen and A. Pasquarello, Phys. Rev. B **92**(Jul), 041115 (2015).

[21] M. Shishkin, M. Marsman, and G. Kresse, Phys. Rev. Lett. **99**(Dec), 246403 (2007).

[22] A. Zunger, S. H. Wei, L. G. Ferreira, and J. E. Bernard, Phys. Rev. Lett. **65**(Jul), 353–356 (1990).

[23] W. R. L. Lambrecht, C. Bhandari, and M. van Schilfgaarde, Phys. Rev. Materials **1**(Sep), 043802 (2017).

[24] B. Liu, M. Gu, and X. Liu, Appl. Phys. Lett. **91**(17), 172102 (2007).